Fine-structure investigation of gamma-irradiated poly(γ-benzyl-L-glutamate) (*DP* 1460) by small-angle X-ray scattering using correlation functions

T. Misra*, S. Rath, T. Patel, N. V. Bhatt† and D. K. Bisoyi‡
Department of Physics, RE College, Rourkela 769008, Orissa, India
(Received 9 June 1993; revised 23 September 1993)

A small-angle X-ray scattering (SAXS) study has been carried out to show the changes that occur in the macromolecular structure of poly(γ-benzyl-L-glutamate) (PBLG) with degree of polymerization 1460, when it is subjected to different doses of γ-radiation. It has been observed that the SAXS profiles of various samples undergo drastic changes with increase in dose and their tail regions show a deviation from Porod's law, which indicates that they are non-ideal two-phase structures, characterized by continuous variation of electron density at the phase boundary. The three- and one-dimensional correlation functions have been computed from the background-corrected SAXS profiles, and various macromolecular parameters have been evaluated following the theories of Vonk and Ruland for non-ideal two-phase structures.

(Keywords: poly(γ-benzyl-L-glutamate); macromolecular structure; gamma irradiation)

INTRODUCTION

The presence of molecular clusters in the polypeptide poly(γ-benzyl-L-glutamate) (PBLG) enables it to be conveniently handled for its fine-structure investigation by small-angle X-ray scattering.

Small-angle X-ray scattering (SAXS) profiles obtained from ideal two-phase systems with sharp boundaries have been treated by Porod[1,2], where it was observed that the product $\tilde{I}(\theta)\theta^3$ comes out to be a constant at large scattering angle. Here, θ is half the scattering angle and $\tilde{I}$ is the smeared-out intensity. Work on polymers often exhibits systematic deviations from Porod's law, where the above product does not reach a constant value at large θ, causing enhancement of scattering at high angles and leading to a positive slope of $\tilde{I}(\theta)\theta^3$ *versus* θ^2, known as a positive deviation from Porod's law. This deviation occurs when the electron density, instead of remaining constant within the phases, may have long-range fluctuations from the mean value in either phase or in both phases. If the size of molecules is very small, SAXS study cannot be carried out. When there is intrusion of a low-angle tail on the main wide-angle peak, the intensity curve reaches a minimum intensity value and then shows a rising trend. Such a trend is not seen in our case. The existence of a diffuse phase boundary, on the other hand, causes a depletion of high-angle scattering, leading to a negative slope for a similar plot. This effect is referred to as a negative deviation from Porod's law[3,4]. Ruland[5] considered that when the phase change is not sharp but occurs over a certain range *E*, known as the width of the transition layer, this negative deviation occurs. This finite width of the density transition is due to corrugation (or roughness) of the surface of the particles[6], giving rise to a large surface area. This results in the absence of weak boundaries, enhancing fracture toughness.

According to Ruland[5], for many systems the phase boundary may not be sharp but characterized by a certain range *E*. Later Vonk[6] developed the practical aspects of Ruland's method, and such systems are referred to as non-ideal two-phase systems. Deviation of Porod's law in terms of a model containing two phases having a diffuse boundary layer in which density varies gradually from one phase to the other is a linear gradient model.

EXPERIMENTAL

Materials

The polypeptide PBLG was obtained from the Department of Functional Polymer Science, University of Shinshu, Japan. The PBLG of degree of polymerization (*DP*) 1460 was supplied by Pilot Chemicals Ltd. (Lot No. G-I4I) and was prepared from the *N*-carboxy-α-amino acid anhydride of γ-benzyl-L-glutamate. It has been pointed out by Iizuka[7] that electrically and magnetically oriented films of polypeptide PBLG have lamellar textures ranging from a few to several micrometres in thickness with lamellae perpendicular to the external field direction. The lamellae are made up of rods or sheets with a diameter or width of about 0.1 μm. The gap regions between two adjacent lamellae have been detected by Iizuka[7] and these observations appear to be strong indications of the presence of molecular clusters. Also Sobajima[8] has pointed out that the orientation of PBLG

---

* To whom correspondence should be addressed at Rourkela Institute of Technology, Kalunga, Rourkela, Orissa, India

† Centre of Advanced Studies (Physics), University Department of Chemical Technology, Matunga, Bombay 19, India

‡ Department of Physics, Gandhi Mahavidyalaya, Rourkela, Orissa, India

0032-3861/94/11/2278–06

in the isotropic state becomes observable in a magnetic field. These properties of PBLG enable it to be conveniently handled for its fine-structure investigation by the small-angle scattering method. In our present work, we have taken PBLG with *DP* 1460 (designated as PBLG-I), which is further irradiated by 1 and 3 Mrad of γ-radiation and designated as PBLG-II and PBLG-III respectively.

X-ray measurements

The small-angle X-ray scattering measurements were made at the Centre of Advanced Studies (Physics), University Department of Chemical Technology, Matunga, Bombay, by means of a compact Kratky camera[9]. The entrance slit and the counter slit attached to the Kratky camera were adjusted at 80 μm and 120 μm respectively. X-ray radiations were obtained from a Philips generator with a copper target operated at 40 kV and 20 mA, and the monochromatization was achieved using a nickel filter of 10 μm thickness. The monochromatic Cu K_α ($\lambda = 1.54$ Å) radiation thus obtained is used to irradiate the samples by inserting them in Mark capillary tubes of 1 mm diameter. To reduce the scattering of X-rays by air between the sample and detector, vacuum in the intervening space was maintained at a pressure of about 0.5 mbar. The distance of the sample to the detector *a* was kept at 20 cm.

THEORY

In case the absolute intensities are not available, a parameter, *R* (ref. 10), which is very useful for the characterization of structure, is given by (see Appendix for symbols):

$$R = \frac{\langle |\mathrm{grad}\,\eta|^2 \rangle}{\langle \eta^2 \rangle} = 6\pi^2 \frac{\int_0^\infty s^3 \tilde{I}(s)\,\mathrm{d}s}{\int_0^\infty s\tilde{I}(s)\,\mathrm{d}s} \tag{1}$$

In an ideal two-phase structure, the gradient at the phase boundary is infinite, and consequently *R* goes to infinity. On the other hand, if *R* is finite the electron density changes from one phase to the other continuously over a region *E*. This relation (1) for *R* has been transformed to variable *x* by Misra *et al.*[10] as:

$$R = \frac{3}{2}\left(\frac{2\pi}{\lambda a}\right)^2 \frac{\int_0^\infty x^3 \tilde{I}(x)\,\mathrm{d}x}{\int_0^\infty x\tilde{I}(x)\,\mathrm{d}x} \tag{2}$$

The value of *R* obtained from (2) determines the nature of the sample, i.e. whether it belongs to an ideal or non-ideal two-phase system.

According to Vonk[6], the relation:

$$\langle |\mathrm{grad}\,\eta|^2 \rangle = (\Delta\eta)^2 S/E_\mathrm{V} V \tag{3}$$

holds for a pseudo-two-phase structure. According to Debye *et al.*[11], *S*/*V* for a two-phase structure can be found from the slope of the three-dimensional correlation function at the origin given by:

$$\left[\frac{\mathrm{d}C(r)}{\mathrm{d}r}\right]_{r=0} = -\left(\frac{S}{4V}\right)\left(\frac{(\Delta\eta)^2}{\langle \eta^2 \rangle}\right) \tag{4}$$

This relation may also be applied to pseudo-two-phase structures, provided the slope is taken at a distance of at least *E* Å away from the origin. Combination of (1), (3) and (4) then leads to:

$$E_\mathrm{V} = -\frac{4}{R}\left[\frac{\mathrm{d}C(r)}{\mathrm{d}r}\right]_{r=E_\mathrm{V}} \tag{5}$$

To calculate E_V, one has to evaluate the values of *C*(*r*), the three-dimensional correlation function at various values of *r* in real space. It has been established by Mering and Tchoubar[12] that *C*(*r*) can be calculated from the expression

$$C(r) = \frac{\int_0^\infty s\tilde{I}(s) J_0(2\pi r s)\,\mathrm{d}s}{\int_0^\infty s\tilde{I}(s)\,\mathrm{d}s} \tag{6}$$

The above expression for *C*(*r*) can be written in terms of *x* as:

$$C(r) = \frac{\int_0^\infty x\tilde{I}(x) J_0(2\pi r x/\lambda a)\,\mathrm{d}x}{\int_0^\infty x\tilde{I}(x)\,\mathrm{d}x} \tag{7}$$

Again the one-dimensional correlation function $C_1(y)$ for a lamellar system given by Mering and Tchoubar[12] when changed to *x* variable reduces to:

$$C_1(y) = \frac{\int_0^\infty x\tilde{I}(x)[J_0(z) - zJ_1(z)]\,\mathrm{d}x}{\int_0^\infty x\tilde{I}(x)\,\mathrm{d}x} \tag{8}$$

where $z = 2\pi x y/\lambda a$.

It was shown by Vonk[6] that the position of the first subsidiary maximum in the one-dimensional correlation function gives the value of *D*. The relation

$$\left[\frac{\mathrm{d}C_1(y)}{\mathrm{d}y}\right]_{y>E} = -\left(\frac{1}{D}\right)\left(\frac{(\Delta\eta)^2}{\langle \eta^2 \rangle}\right) \tag{9}$$

derived by Vonk can be used to calculate the value of $(\Delta\eta)^2/\langle\eta^2\rangle$. Here the slope is taken at a point where *y* is greater than *E*.

It has been proved by Vonk[6] that the second differentials of *C*(*r*) and $C_1(y)$ at the origin are given by the relation:

$$\left[\frac{\mathrm{d}^2 C_1(y)}{\mathrm{d}y^2}\right]_{y=0} = 3\left[\frac{\mathrm{d}^2 C(r)}{\mathrm{d}r^2}\right]_{r=0} \tag{10}$$

For a layer structure, as shown by Vonk[6], the specific inner surface, *S*/*V*, can be written as:

$$S/V = 2/D \tag{11}$$

For a non-ideal two-phase structure, the following relation holds[6]:

$$\frac{\langle \eta^2 \rangle}{\langle (\Delta\eta)^2 \rangle} = [\phi_1\phi_2 - (S/V)(E/6)] \tag{12}$$

Assuming the sum of ϕ_1 and ϕ_2 to be unity, the values of ϕ_1 and ϕ_2 can be determined from relation (12).

According to Mittelbach and Porod[13] and Porod[2], $\bar{l}_1$ and $\bar{l}_2$ are given by:

$$\bar{l}_1 = 4\phi_1 V/S \tag{13}$$

$$\bar{l}_2 = 4\phi_2 V/S \tag{14}$$

with $\bar{l}_r$ as

$$1/\bar{l}_r = 1/\bar{l}_1 + 1/\bar{l}_2 \tag{15}$$

As given by the above workers, l_c for a specimen is:

$$l_c = 2\int_0^\infty C(r)\,\mathrm{d}r \tag{16}$$

The method for estimating the value of E has been given by Ruland[14]. The functional relation of $\tilde{I}(s)$ with s at the tail end of the SAXS pattern, for a non-ideal two-phase system, is given by:

$$\tilde{I}(s\rightarrow\infty) = \frac{\pi c}{2}\left[\frac{1}{s^3} - 2\pi^2\left(\frac{E^2}{3s}\right)\right] \tag{17}$$

For an ideal two-phase structure, $E=0$, hence the above equation reduces to Porod's law. When transformed to x variable, the above relation becomes:

$$\tilde{I}(x\rightarrow\infty)x = \frac{\pi c(\lambda a)^3}{2}x^{-2} - \frac{\pi^3 c}{3}(\lambda a)E^2 \tag{18}$$

The value of E_R can be obtained from the graph of $\tilde{I}(x)x$ *versus* x^{-2}, commonly known as a Ruland plot.

BACKGROUND CORRECTION

All the SAXS intensities, in principle, are superimposed on a continuous sample background sometimes known as fluctuation scattering or liquid scattering and different from parasitic scattering. For accurate quantitative interpretation of the observed SAXS data, it is absolutely necessary to find out the background scattering for the whole observed range, and it should be properly treated and dealt with, since the correlation function at the origin is very sensitive to any error in the tail end of the scattering curve[6]. Therefore, special care must be taken to separate the SAXS intensity $\tilde{I}(x)$ from the continuous background scattering $\tilde{I}_{bg}(x)$ (ref. 6).

As reported by Kortleve *et al.*[15] the continuous background in some SAXS patterns shows an upward trend at large values of x after a minimum is attained in the SAXS curve, and in such a case, the experimentally observed data at the tail end region can be fitted to an equation of the type:

$$\tilde{I}_{bg}(x) = a + bx^n$$

where a, b are constants and n is an even positive integer. However, it was shown by Konrad and Zachmann[16]

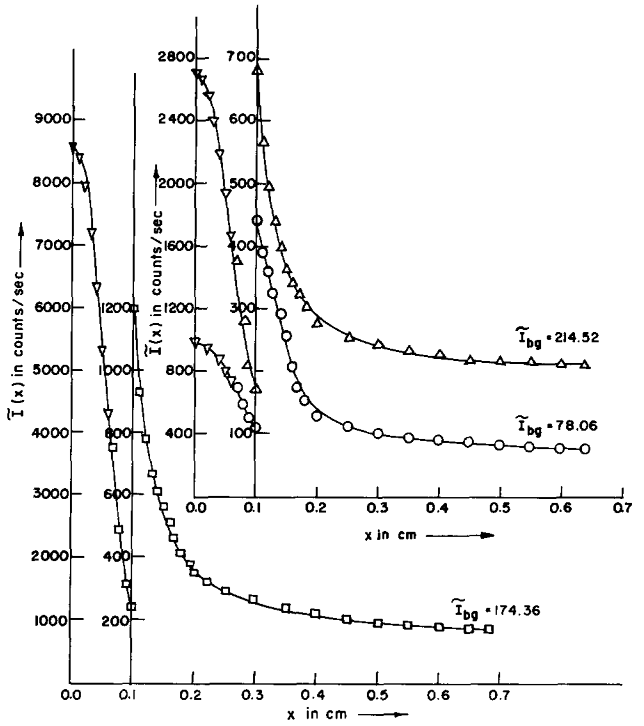

Figure 1 Smeared-out scattering profiles for PBLG-I (○), PBLG-II (1 Mrad) (□) and PBLG-III (3 Mrad) (△), magnified from $x=0.1$ cm. The extrapolated points are shown by inverted triangles (▽)

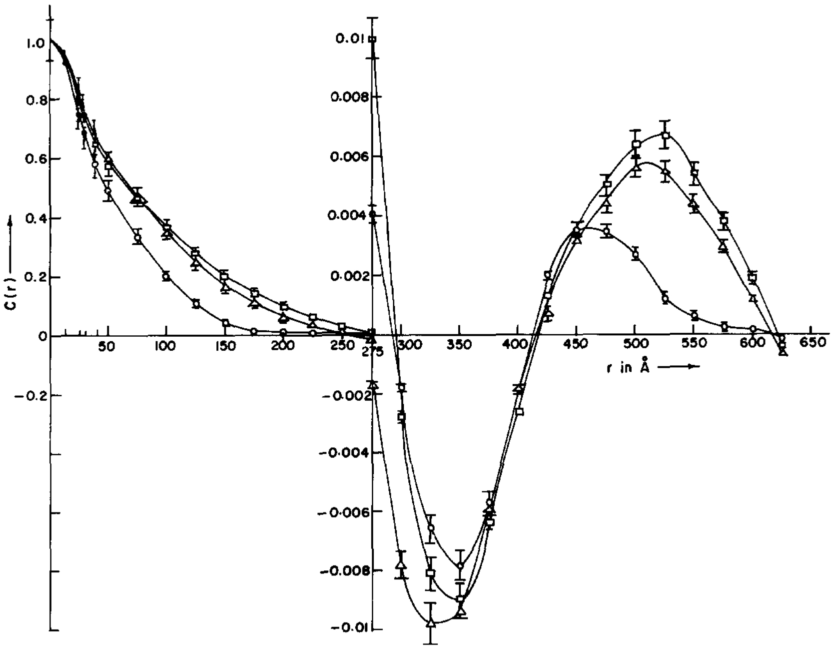

Figure 2 Curves of the three-dimensional correlation functions $C'(r)$ against r with error bars: PBLG-I (○), PBLG-II (1 Mrad) (□) and PBLG-III (3 Mrad) (△), magnified from $r=275$ Å

that $\tilde{I}_{bg}(x)$ remains constant in the region where $\tilde{I}(x)$ contributes appreciably. For both the assumptions corresponding to background intensities, the value of E, when calculated following the methods of Vonk and Ruland, shows only a relatively small difference. So one is justified in deducting a constant background intensity corresponding to a minimum intensity value in the SAXS pattern[10] as is done in our case. These background-corrected SAXS intensities have been used in subsequent analysis, with 5% statistical error in intensity data as observed by our experimental study. The effect of this error has been taken care of in subsequent calculation of correlation function and error bars have been plotted. At appropriate places, the limits of errors resulting from the intensity fluctuation have been incorporated while evaluating the various parameters. In our work, constant background intensities marked as $\tilde{I}_{bg}$ in *Figure 1* are deducted.

APPLICATIONS AND RESULTS

Five intensity values near the origin were fitted to the Gaussian curve[17]:

$$\tilde{I}(x \to 0) = p\exp(-qx^2)$$

by least-squares technique and the values of constant p obtained are 986.53, 8589.05 and 2711.91 J m^{-2} s^{-1} respectively and of q are 78.70, 191.22 and 134.72 m^{-2} for PBLG-I, PBLG-II and PBLG-III respectively. Taking these values of p and q, the scattering curves for the three samples were extrapolated and are shown in *Figure 1*. It may be noted here that this extrapolation has very little effect on the relevant part of the correlation functions. Neither the position nor the height of the first subsidiary maximum of the one-dimensional correlation function is much affected[10].

Using relation (7), the three-dimensional correlation function $C(r)$ was computed for various values of r and are shown in *Figure 2* for the three samples with error bars. As per Vonk[6], the relation $R = -3[\mathrm{d}^2C(r)/\mathrm{d}r^2]_{r=0}$ is valid for an isotropic sample. In our case the values of $-3[\mathrm{d}^2C(r)/\mathrm{d}r^2]_{r=0}$ for the three samples were

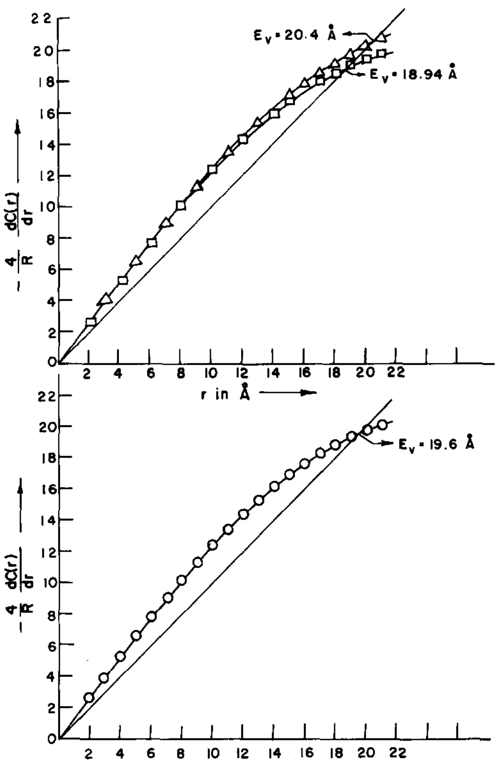

Figure 3 Curves of $-(4/R)\,\mathrm{d}C(r)/\mathrm{d}r$ against r values: PBLG-I (○), PBLG-II (□) and PBLG-III (△)

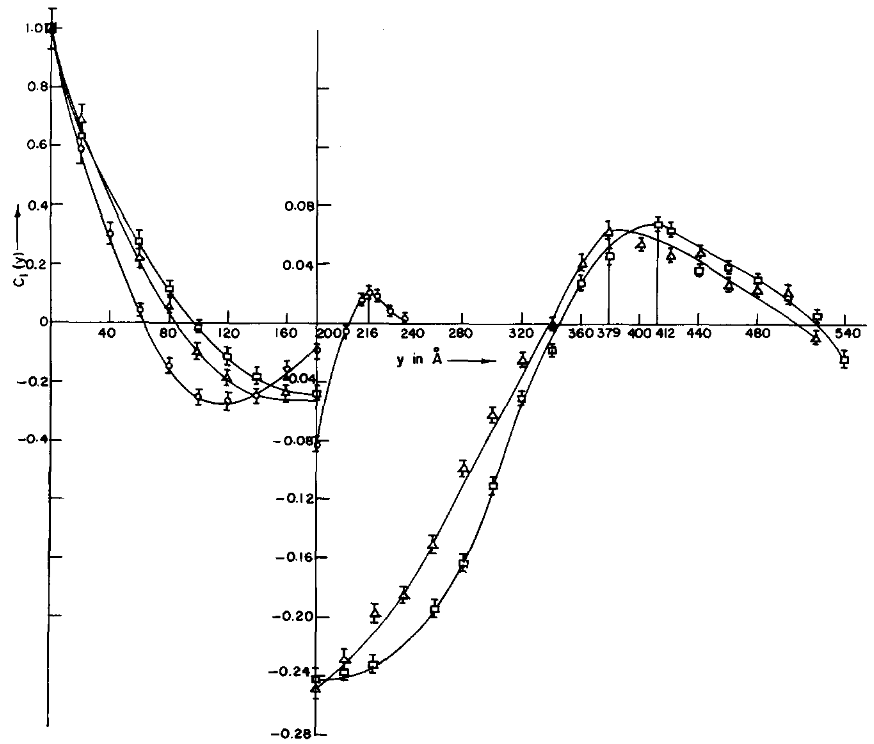

Figure 4 Curves of the one-dimensional correlation functions $C_1(y)$ against y values with error bars: PBLG-I (○), PBLG-II (□) and PBLG-III (△), magnified from $y = 180$ Å

Table 1

Parameters	PBLG-I	PBLG-II	PBLG-III
$\bar{l}_1$ (Å)	330.63±2.51	721.77±6.61	647.0±6.96
$\bar{l}_2$ (Å)	101.37±2.51	102.23±6.61	111.01±6.96
$\bar{l}_r$ (Å)	77.58±1.06	89.55±2.18	94.75±2.46
$\bar{l}_c$ (Å)	124.0±0.92	177.0±1.05	167.0±1.05
S/V(Å^{-1})	9.26×10^{-3}	4.85×10^{-3}	5.28×10^{-3}
D (Å)	216	412	379
ϕ_{12}	0.179±0.004	0.108±0.003	0.125±0.003
ϕ_1 (%)	76.5±0.6	87.6±0.8	85.3±0.9
ϕ_2 (%)	23.5±0.6	12.4±0.8	14.6±0.9
R (Å^{-2})	$(2.65\pm0.19)\times10^{-3}$	$(2.35\pm0.16)\times10^{-3}$	$(1.99\pm0.14)\times10^{-3}$
E_R (Å)	18.44±0.02	17.36±0.01	18.53±0.01
E_V (Å)	19.6±1.16	18.94±1.36	20.40±1.5

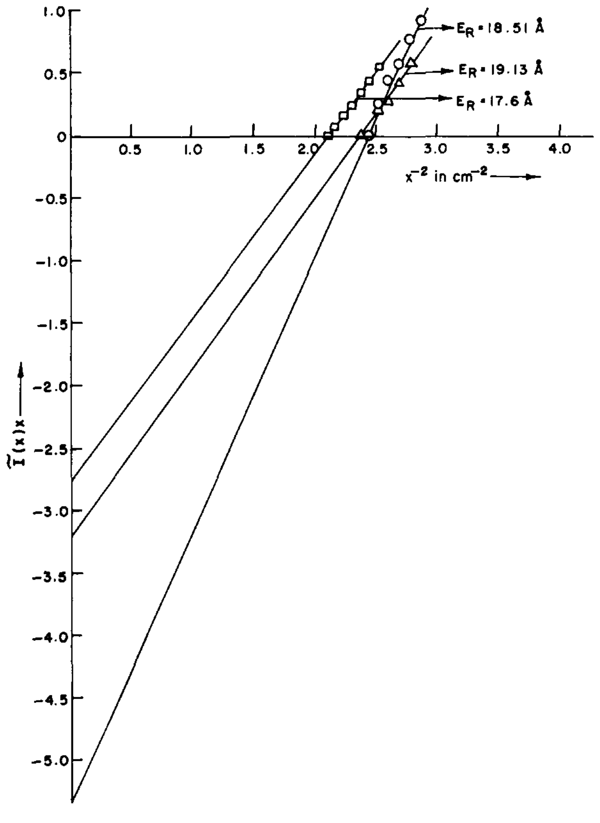

Figure 5 Ruland plot of $\tilde{I}(x)x$ *versus* x^{-2}: PBLG-I (○), PBLG-II (□) and PBLG-III (△)

found to be $(2.66\pm0.30)\times10^{-3}$, $(2.36\pm0.29)\times10^{-3}$ and $(1.99\pm0.12)\times10^{-3}$ Å^{-2} for PBLG-I, PBLG-II and PBLG-III respectively, which are in good agreement with the R values, indicating that the samples are isotropic. The slope of $C(r)$ of each sample at different points was computed by numerical differentiation, applying the five-point central difference formula with a regular interval of 1 Å. The values of $-(4/R)\,(\mathrm{d}C(r)/\mathrm{d}r)$ *versus* r for each sample are plotted in *Figure 3*. The values referred to as E_V, for the three samples, are also shown in the figure.

As shown by Iizuka[7], PBLG has a layer structure, and therefore the one-dimensional correlation function $C_1(y)$ applicable for a layer structure was calculated for each sample using relation (8) for various values of y.

The values of $C_1(y)$ *versus* y values with error bars are shown in *Figure 4* for the three samples. The values of D were found by noting the position of the first subsidiary maximum in each curve in *Figure 4*. The 5% fluctuation in the intensity data in case of a sample produces no change in the position of the first subsidiary maximum as verified by the computation of $C_1(y)$.

The plots of $\tilde{I}(x)x$ *versus* x^{-2} of each of the samples are shown in *Figure 5*. The plots give straight lines at the limiting region of the scattering curves. The values of standard deviation of intensities $\sigma(\tilde{I})^{1/2}$ at the tail end of the SAXS pattern were found to be 0.02, 0.002 and 0.01 for PBLG-I, PBLG-II and PBLG-III respectively, which are well within the permissible limits. The coefficient of the line of regression, γ, for the three samples was computed as 0.91, 0.87 and 0.86 for PBLG-I, PBLG-II and PBLG-III respectively, which were close to unity, suggesting more or less the correctness of the data.

Other calculations were made on the above theories and the results obtained are displayed in *Table 1*.

DISCUSSION AND CONCLUSION

Correctness of data

The values of standard deviation of intensities $\sigma(\tilde{I})^{1/2}$ at the tail end of the SAXS pattern of each sample were found to be much less than 0.5, indicating the correctness of data[18]. Further, the coefficient of the line of regression, γ, was also close to unity for each sample, suggesting more or less the statistical correctness of the data[19].

Also the approximately equal values of E_V, due to Vonk, and E_R, due to Ruland, confirm the correctness of the data collection and the method of analysis.

PBLG belongs to a non-ideal two-phase structure

It has been mentioned earlier that for an ideal two-phase structure, the intercept of the Ruland plot vanishes, leading to application of Porod's law. When this intercept is negative, as in our case, the system is considered to be a non-ideal two-phase system. So PBLG comes under non-ideal two-phase systems.

The value of $C(r)$ initially remains positive and comes to zero for a dilute system at large values of r (ref. 20). But in the case of a non-ideal two-phase system, the $C(r)$ function oscillates at large values of r as shown in *Figure 2*.

Effect of γ-radiation

When PBLG-I is exposed to 1 Mrad of γ-radiation, the D value increases as compared to PBLG-I. This may be due to the crosslinking of PBLG, as a result of which the interlayer transverse periodicity increases and the matter phase becomes thicker. But when PBLG-I is subjected to 3 Mrad of γ-radiation, the D value decreases, leading to the increase of specific inner surface, S/V. This may be due to the breakdown of molecules, i.e. degradation[21].

ACKNOWLEDGEMENTS

We thank Professor S. Misra, Principal, RE College, Rourkela, for granting permission to use the computer and other facilities of the Physics Department. We are also grateful to Dr K. C. Patra and S. S. Khuntia for their help during the progress of the work.

REFERENCES

1 Porod, G. *Kolloid Z.* 1951, **124**, 83
2 Porod, G. *Kolloid Z.* 1952, **125**, 51
3 Helfand, E. *Acc. Chem. Res.* 1975, **8**, 295
4 Helfand, E. and Tagmi, V. *Polym. Lett.* 1971, **9**, 741
5 Ruland, W. *J. Appl. Crystallogr.* 1971, **4**, 70
6 Vonk, C. G. *J. Appl. Crystallogr.* 1973, **6**, 81
7 Iizuka, E. *Adv. Polym. Sci.* 1976, **20**, 79
8 Sobajima, S. *J. Phys. Soc. Japan* 1967, **23**, 1070
9 Kratky, O. 'Small Angle X-ray Scattering' (Ed. H. Brumberger), Gordon and Breach, New York, 1967
10 Misra, T., Patra, K. C. and Patel, T. *Colloid Polym. Sci.* 1984, **262**, 611
11 Debye, P., Anderson, H. R. and Brumberger, H. *J. Appl. Phys.* 1957, **28**, 279
12 Mering, J. and Tchoubar, D. *J. Appl. Crystallogr.* 1965, **1**, 153
13 Mittelbach, P. and Porod, G. *Kolloid Z. Z. Polym.* 1965, **202**, 40
14 Ruland, W. *Colloid Polym. Sci.* 1977, **255**, 417
15 Kortleve, G., Tuynman, C. A. F. and Vonk, C. G. *Polym. Sci.* (*A2*) 1972, **10**, 123
16 Konrad, G. and Zachmann, N. G. *Kolloid Z. Z. Polym.* 1971, **247**, 851
17 Vonk, C. G. *J. Appl. Crystallogr.* 1975, **8**, 340
18 Vonk, C. G. *J. Appl. Crystallogr.* 1971, **4**, 341
19 Topping, J. 'Errors of Observation and Their Treatment', 4th Edn., Chapman and Hall, London, 1972
20 Guinier, A. and Fournet, G. 'Small Angle Scattering of X-rays', Wiley, New York, 1955, p. 79
21 Wang, C. S. and Yesh, G. S. Y. *J. Macromol. Sci.–Phys.* (*B*) 1981, **20** (1), 101

APPENDIX

Glossary of symbols

c	proportionality constant
D	average periodicity transverse to the layer
E	width of transition layer
E_R	width of transition layer as determined by Ruland's method[5]
E_V	width of transition layer as determined by Vonk's method[6]
$J_0(z)$	Bessel function of zero order of the first kind for argument z
$J_1(z)$	Bessel function of first order of the first kind for argument z
$\bar{l}_1$	transverse length in the matter region
$\bar{l}_2$	transverse length in the void region
l_c	coherence length
l_r	range of inhomogeneity
R	a constant in the characterization of structure
S	total surface area of the matter phase
s	coordinate in Fourier space ($s = 2\theta/\lambda$)
V	total volume of the irradiated sample
x	position coordinate of the scattered intensity from the centre of the primary beam
η	deviation of electron density from the mean value
$\Delta\eta$	electron density difference of the two phases
ϕ_1	volume fraction of matter phase
ϕ_2	volume fraction of void phase
θ	half the scattering angle ($2\theta = x/a$)
λ	wavelength